

Personalized Restoration via Dual-Pivot Tuning

Pradyumna Chari^{1,†} Sizhuo Ma² Daniil Ostashev² Achuta Kadambi¹
 Gurunandan Krishnan² Jian Wang^{2,*} Kfir Aberman²
¹University of California, Los Angeles ²Snap Inc.

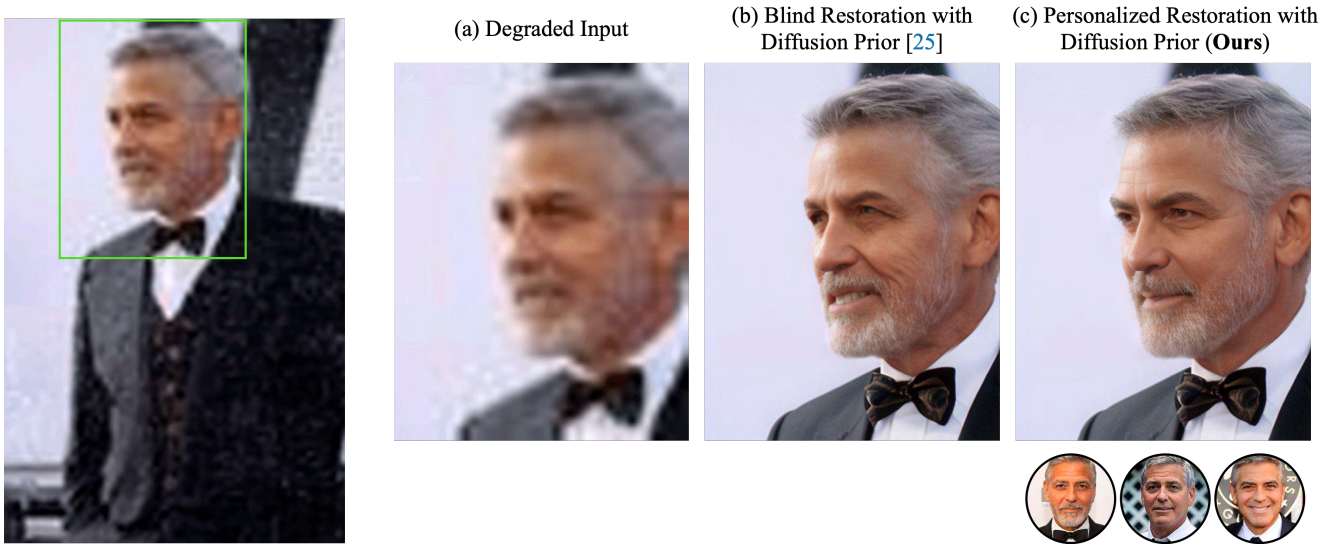


Figure 1. Given a degraded image of an individual’s face (a), diffusion-based blind restoration approaches [25] may not retain the individual’s identity (b). However, with a few reference images (bottom right), our *dual-pivot tuning* technique (c) can reconstruct the face while maintaining high identity fidelity to the individual and without any perceivable loss in fidelity to the degraded input.

Abstract

Generative diffusion models can serve as a prior which ensures that solutions of image restoration systems adhere to the manifold of natural images. However, for restoring facial images, a personalized prior is necessary to accurately represent and reconstruct unique facial features of a given individual. In this paper, we propose a simple, yet effective, method for personalized restoration, called *Dual-Pivot Tuning* — a two-stage approach that personalize a blind restoration system while maintaining the integrity of the general prior and the distinct role of each component. Our key observation is that for optimal personalization, the generative model should be tuned around a fixed text pivot, while the guiding network should be tuned in a generic (non-personalized) manner, using the personalized generative model as a fixed “pivot”. This approach ensures that personalization does not interfere with the restoration pro-

cess, resulting in a natural appearance with high fidelity to the person’s identity and the attributes of the degraded image. We evaluated our approach both qualitatively and quantitatively through extensive experiments with images of widely recognized individuals, comparing it against relevant baselines. Surprisingly, we found that our personalized prior not only achieves higher fidelity to identity with respect to the person’s identity, but also outperforms state-of-the-art generic priors in terms of general image quality. Project webpage: <https://personalized-restoration.github.io>

1. Introduction

Image restoration is an extensively researched problem, characterized by its inherent ill-posed nature. The goal of the restoration task is to find visually plausible and natural images that maintain perceptual fidelity to the degraded input image [47]. In blind restoration scenarios where no

[†]Work partially done during an internship at Snap Inc.

^{*}Corresponding author

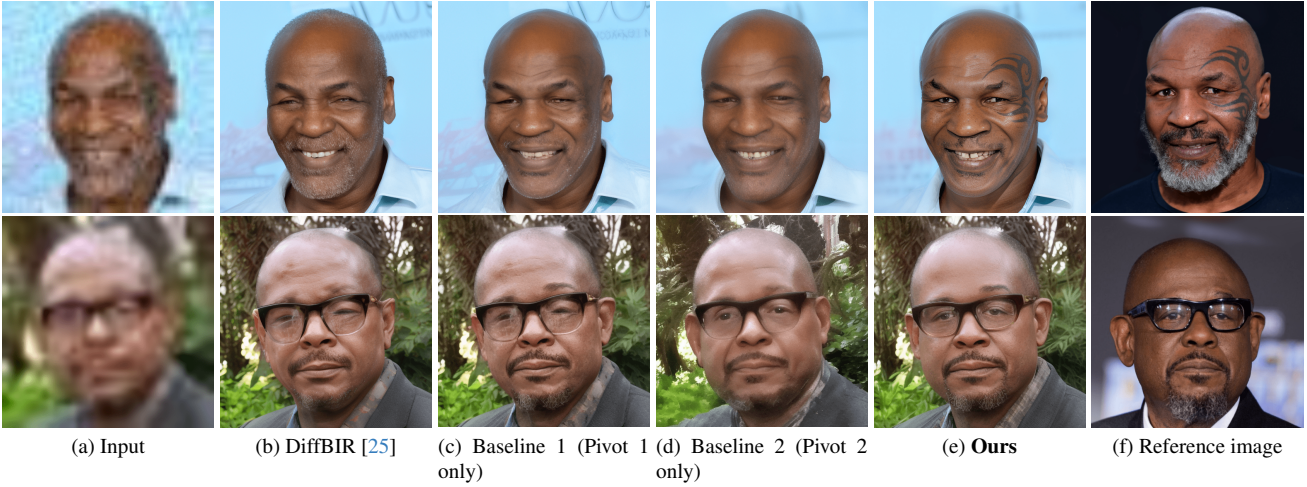


Figure 2. **Restoration Baselines.** Given a real, degraded input image (a) features a person whose identity is referenced in another image (f), a diffusion-based blind restoration method [25] with a general (non-personalized) prior, fails to preserve the person’s identity (b). When fine-tuning the text-to-image prior with a text pivot only [35], the system ignores the personalized generator when reintegrated into the system (c), while personalizing the feature encoder with the generative model as a pivot only leads to lack of detail in the result (tattoo in the first row, detail such as beard, general high frequencies in the second row), along with absence of generalization across identities (d). In contrast, our method (e) effectively incorporates the individual’s identity into the restoration process while retaining a quality comparable to the base model (b).

prior information about the subject or the degradation is available, a prior describing the manifold of natural images is needed. However, for face image restoration, having an identity prior is necessary to ensure that the output image remains within a manifold that accurately represents the distinctive facial features of the individual in the degraded image. This sets the basis for prior work in reference-based face image restoration [23, 24, 29].

Text-to-Image Diffusion Models [34, 37] have revolutionized image synthesis, enabling the generation of images from textual descriptions. These models act as versatile generative priors for various downstream tasks, and were recently explored in the context of blind image restoration, enhancing the naturalness of restored images [25, 43]. Moreover, the ability to personalize these diffusion models with just a few reference images opens new avenues for tailored content creation [13, 35]. Despite these advancements, effectively integrating personalization into a diffusion-based blind restoration systems remains an open challenge.

To highlight the challenges associated with personalizing a blind restoration system, Fig. 2 demonstrates how naive personalization approaches fall short. As shown in Fig. 2 (c), a personalized text-to-image model that simply replaces the general one in a blind restoration system can be disregarded by the unconditional system. Alternatively, naive personalization of the image conditioning encoder (from [25], for example) disrupts the natural image prior, leading to a lack of detail in the restored image as demonstrated in Fig. 2 (d).

In this paper, we propose a simple technique for personalizing a text-to-image prior within the context of a blind

image restoration framework. Given a small set (~ 10) of high-quality images of a person, our goal is to restore their other degraded images, ensuring that the results exhibit (1) high fidelity to the identity of the person, (2) high fidelity to the degraded image, (3) natural appearance.

Our key idea, coined *dual-pivot tuning*, is to fine-tune the prior within the context of a blind image restoration system, while preserving the integrity of the general prior and the distinct roles of each component within the system. Specifically, we propose a two-step solution, to personalize a general blind image restoration system which consists of two main components: a diffusion-based generative prior, and a guiding image encoder.

In the first step, we personalize the diffusion-based generative prior in the context of the blind restoration system, while using a text prompt (for example, “a photo of a [v] man”) as a *textual pivot* - a fixed token that is held constant during the fine-tuning process [35]. However, in our case the fine-tuning is performed with the guiding image encoder such that the personalized prior learns to respect the attributes of the guiding image. In the second step, we fine-tune the guiding encoder to align with the personalized, “shifted”, prior of the diffusion model, thereby retargeting its functionality. During this phase, we aim to maintain the identity-agnostic nature of the encoder, allowing its applicability across various personalized models. Therefore, we fine-tune it with general face images (not of the specific individual). We refer to the fixed personalized network as a pivot, around which we adjust the weights of the guiding encoder.

We find both of these operations, in this sequence, to be essential. While the textual pivot enables identity injection

without losing the general face prior of the base model in the restoration system, fine-tuning around the network pivot leads to better utilization of the guiding encoder and higher fidelity to the input image features. Furthermore, we leverage the diffusion process’s characteristics, noting that identity formation occurs later in the process, where it primarily shapes finer details rather than the initial, noisier phase that sets coarse image features. Our approach demonstrates that personalization can be effectively applied at specific stages of the diffusion process which can reduce the expansive fine-tuning time by approximately $\times 2$.

We compare our method against few-shot learning baselines and evaluate them using publicly available images of well-known figures, leveraging our pre-existing knowledge of their features. Our experimenters shows that our method reconstruct key facial features of the subject in the reference images while maintaining high fidelity to the original degraded image, outperforming others quantitatively and qualitatively. Moreover, user studies, interestingly, confirm that this personalization aspect contributes significantly not only to identity preservation but also to the perceived overall quality improvement of the generated images. Fig. 1 shows one example that demonstrates how our method is able to surpass existing diffusion-based blind face restoration methods [25] in terms of identity retention while maintaining the same quality of face image restoration.

To the best of our knowledge, this is the first approach to leverage a personalized diffusion prior for restoration tasks.

2. Related Work

2.1. Blind Face Image Restoration

Distinct from general scene image restoration, face image restoration typically leverages facial priors to achieve superior results. Depending on how these facial priors are utilized, previous methods can be broadly categorized into three main classes. (1) Geometric prior: These approaches incorporate geometric cues, such as facial landmarks [5, 9, 19], parsing maps [7, 38, 50], and component heatmaps [52], into the network’s design. (2) Dictionary prior: In this method, a dictionary is first learned from a collection of face images, either in the image space [21] or feature space [15, 48, 55, 56]. Subsequently, a degraded image is reconstructed using high-quality words from this dictionary. (3) Generative prior: This category encompasses techniques like GAN (Generative Adversarial Network) prior [6, 27, 46, 51] or diffusion prior [25, 49, 53]. Among these methods, approaches falling under categories (2) and (3) have demonstrated the most promising results. Notable algorithms in this context include GFP-GAN [46], CodeFormer [56], and DiffBIR [25].

However, blind face image restoration faces a significant challenge known as the quality-fidelity tradeoff [25, 56].

This arises from the inherent limitations in the information available in the original image. Striking the right balance between generating high-quality results while staying faithful to the original image can be a delicate task. Generating results with too little modification may not yield a significant improvement in quality, while excessive generation can lead to a departure from the identity of the original image. Our proposed method differs from these methods: using personalized diffusion-based methods, we are able to push the tradeoff frontiers by achieving restoration quality while retaining fidelity with respect to identity.

2.2. Reference-Based Face Image Restoration

A high-quality reference image of the same person can greatly benefit face image restoration and help avoid the need of the tradeoff. Depending on the number of references used, such methods can be divided into two categories. (1) Single-reference methods: Examples include GFRNet [20] and GWAINet [12]. (2) Multi-reference methods: Examples include ASFFNet [23], Wang *et al.* [44], and DMDNet [24] (≤ 10 reference images), and MyStyle [29] (~ 100 images). It is evident that multi-reference approaches yield superior results as they leverage more information. Notably, ASFFNet [23] selects an optimal guidance, Wang *et al.* [44] employs pixel-wise weights for multiple references, and DMDNet [24] constructs a dictionary from multiple references; MyStyle [29], on the other hand, fine-tunes StyleGAN based on personal images.

Our proposed method also utilizes multiple reference images to aid personalized restoration. However, there are several distinctions. We use a diffusion-based personalized generative prior, while [12, 20, 23, 44] use feedforward architectures. On the other hand, [29] uses a GAN-based prior, however it requires on the order of 100 images for effective personalization and strict spatial alignment of the face landmarks within each image, while our method is able to operate with 10 reference images and has no restriction on the alignment, operating directly on images in the wild. These distinctions lead to higher quality restoration with less restrictions for our proposed method.

2.3. Personalized Diffusion Models

Diffusion models [11, 17, 39] have notably excelled in the area of generating images from text (T2I) [32, 34, 37] and many other visual computing tasks [31]. Recent advancements in this field involve customization of these established model through fine-tuning, aiming to enhance features like controllability, customization, or to cater to specific applications. One approach to customization involves modifying the T2I model itself [8, 35, 40, 41] or the text embedding process [1, 13, 42], using selected images. This allows to personalize the generation of images based on a particular subject or style, driven by textual input. More re-

cently, neurons in a model specific to a concept can be identified and manipulated specifically to enable sparse personalization [26], methods for fast personalization of the model have been proposed [2, 14, 36], and approaches for multi-subject personalization [3, 30]. Alternatively, other methods involve adapting the T2I model to introduce new conditioning factors. These modifications are either for purposes of image modification [4, 18, 45] or for generating more controlled images [28, 54].

In this work, we tackle the task of contextual customization, where the goal is to fine-tune a prior within the context of a system, preserving the distinct roles of each component within the system, while customizing the image prior to a specific subject.

3. Method

In this section, we outline our method for personalizing guided diffusion models. We start by recapitulating the personalization process for text-to-image models and the application of diffusion priors in blind image restoration. Subsequently, we present our dual-pivot tuning: firstly, employing text-based fine-tuning to embed identity-specific information within diffusion priors, and secondly, the necessity of model-centric pivoting to harmonize the guiding image encoder with the integrated personalized priors. This is followed by an exposition on how our method’s inherent characteristics facilitate accelerated per-identity personalization. A high-level summary of the main idea behind our approach is illustrated in Fig. 3.

3.1. Personalizing Text-Guided Diffusion Models

Given a text prompt \mathbf{p} , text-guided denoising diffusion models learn to sequentially denoise samples of random noise $\epsilon \sim \mathcal{N}(\mathbf{0}, \mathbf{I})$ into samples of images \mathbf{x} . During training, a neural network $\epsilon_\theta(\mathbf{x}_t, \mathbf{p})$ is trained to predict ϵ from a noisy version of the image $\mathbf{x}_t = \alpha_t \mathbf{x} + \sigma_t \epsilon$, where α_t and σ_t are noise scheduling parameters, and t refers to the time step in the diffusion process.

A common way to sample the network at inference time is by using the classifier-free guidance technique [16], that sums up a conditional instance of the model together with an unconditional one:

$$\mathbf{G}_\theta(\mathbf{x}, \mathbf{p}) = (1 + w)\epsilon_\theta(\mathbf{x}_t, \mathbf{p}) - w\epsilon_\theta(\mathbf{x}_t, \emptyset), \quad (1)$$

where w is a guidance scale, and \emptyset represents a null-text prompt. These conditional and unconditional branches aim to strike a balance between prompt-fidelity and diversity within the generated images.

Recent work by Ruiz et al. [35] introduced the ability to personalize text-guided diffusion models using a few reference images of a subject, where the personalization is performed by fine-tuning the model around a text anchor

p (typically designed as a “rare token”+“class noun”, such as ‘a [v] dog’), so the identity of the subject can be embedded into the diffusion prior, and utilized once \mathbf{p} appears in the condition during inference. In practice, the weights, θ , are optimized by minimizing

$$\mathcal{L}_{\text{DB}} = \mathbb{E}_{\mathbf{x}, \mathbf{p}, \epsilon, \epsilon', t} [\|\mathbf{G}_\theta(\mathbf{x}_t, \mathbf{p}) - \epsilon\|_2^2 + \|\mathbf{G}_\theta(\mathbf{x}_t^{\text{pr}}, \mathbf{p}^{\text{pr}}) - \epsilon'\|_2^2], \quad (2)$$

where \mathbf{x}_t^{pr} is drawn from a separate, prior preservation dataset, and \mathbf{p}^{pr} is the prior prompt (“class noun”, such as ‘a dog’). This structure allows the optimization to revolve around a text pivot \mathbf{p} , without ruining the general prior of the model [33].

We define the personalization operator of text-to-image diffusion models by

$$\mathbf{M}_{\mathcal{W}} = \mathcal{P}\{\mathbf{M}, \mathcal{W}\}, \quad (3)$$

where $\mathcal{P}\{\cdot\}$ is the operator, and $\mathbf{M}_{\mathcal{W}}$ is the personalized version of a model \mathbf{M} which is fine-tuned with \mathcal{W} as a pivot. In our case, this pivot can be both a text prompt or a network, as discussed subsequently.

3.2. Diffusion-Guided Image Restoration

Recent advances in blind face image restoration [25, 43] have attempted to utilize a pretrained diffusion model (such as Stable Diffusion [34]) as generative prior to guide the restoration process. Commonly, these pipelines contain a diffusion-guided image restoration step that consist of two components: (1) A general image prior in the form of text-to-image diffusion model $\mathbf{G}(\cdot)$, that encodes the manifold of natural images and (2) an encoder $\mathbf{E}(\cdot)$, that captures context information from the degraded image and guides the generation process such that it maintains high fidelity to the visual attributes of the degraded image. Guiding the diffusion process with spatial features extracted from an image encoder \mathbf{E} is a common way to control the diffusion processes [54]. It should be noted that in case of blind restoration, the general prior \mathbf{G} plays a key role in dictating the identity of the person. As demonstrated in Fig. 4, for a given degraded input image (namely, fixed set of guiding features that are extracted from \mathbf{E}), different seeds in the input of $\mathbf{G}(\cdot)$, lead to different identities in the output.

Our goal in this work is to personalize the general prior \mathbf{G} such that the restored face maintains high fidelity to the identity of the individual without degrading the integrity of the general image prior and the distinct roles of each component in the system.

We consider a general setting, where the encoder $\mathbf{E}(\cdot)$ takes a low-quality image as an input and provides guidance for the diffusion model. That is, the diffusion model receives conditioning from the encoder as well, such that

$$\hat{I} = \mathbf{G}(\epsilon, \mathbf{p}, \mathbf{E}(I_{LQ})), \quad (4)$$

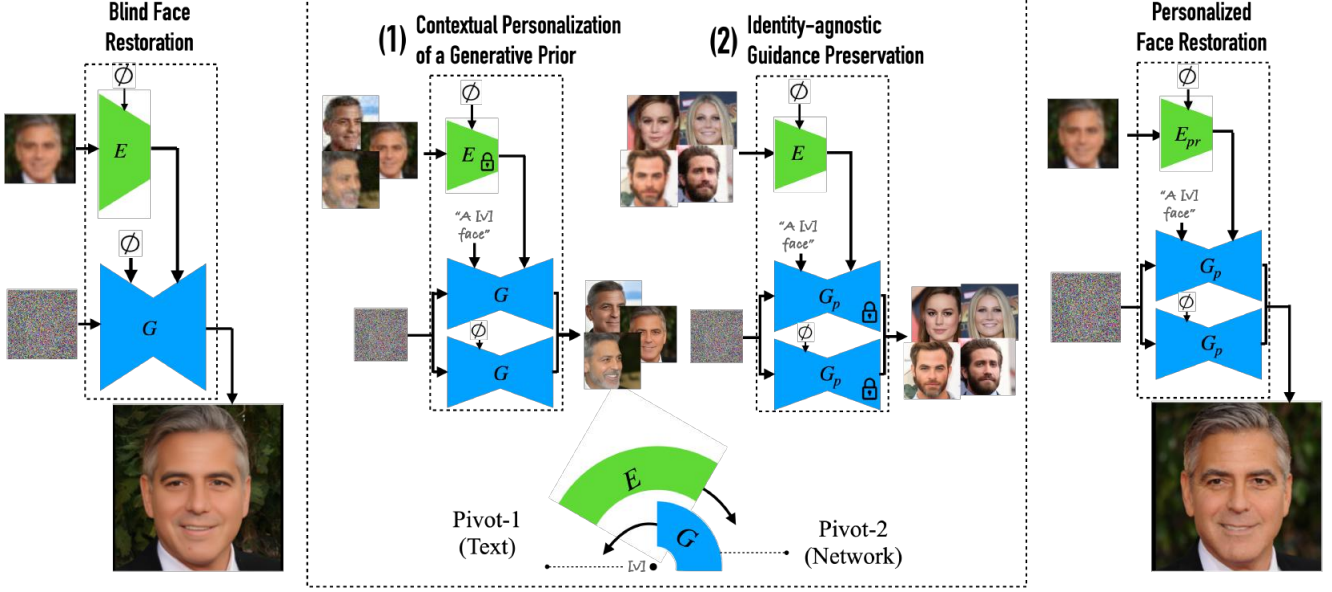


Figure 3. **High-level overview.** Our approach aims to personalize a blind face restoration system (left) and consists of two main steps: (1) text-anchored personalization of the generative prior \mathbf{G} within the context of the system, and (2) adjusting \mathbf{E} in retarget the encoder \mathbf{E} in the presence of the strong personalized prior in \mathbf{G}_p , while guiding the network. Then, at inference time (3), our system embeds the personalized prior and can generate output images with high fidelity to the individual appearing in the reference images.

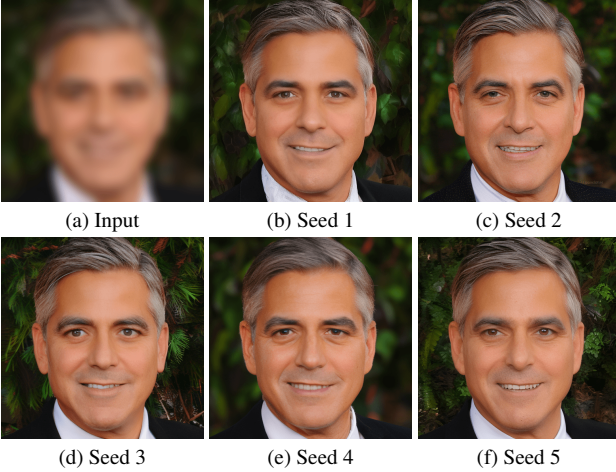


Figure 4. **Identity variation.** Given a fixed degraded input image, it can be seen that different seeds applied to [25] result in images with different identities. Please zoom in closer to observe differences, especially in terms of eyes, teeth and so on.

where I_{LQ} is a low quality image as input and \mathbf{p} is the text conditioning. Note that I_{LQ} could be a degraded image [43], or the output of a preliminary restoration model, like in [25]. In the context of the blind image restoration setting, we will use the following notation:

$$\hat{I} = \mathbf{B}(\mathbf{G}(\epsilon, \emptyset), \mathbf{E}(I_{LQ})), \quad (5)$$

where \mathbf{B} represents the blind restoration system. In this

blind restoration setting, the text conditioning is null (as in [25]).

3.3. Dual-Pivot Tuning

Step-1 - Textual Pivoting. Theoretically, personalization of a generative prior can be decoupled from the context of the system. In our case, we can personalize \mathbf{G} with a pivot text prompt p independently of the blind restoration system and plug it back to the framework, namely,

$$\mathbf{B}_p = \{\mathbf{E}, \mathbf{G}_p\}, \quad (6)$$

where $\mathbf{G}_p = \mathcal{P}\{\mathbf{G}, p\}$. However, as demonstrated in Fig. 2(c), if we do so, the restored images are unable to imbibe identity information and the outputs resemble the images generated with \mathbf{G} , the non-personalized version of the model (Fig. 2(b)).

The occurrence of this issue can be attributed to the initial training of \mathbf{E} , where it was coupled with the unconditional branch of \mathbf{G} . As a result, \mathbf{E} cannot exert influence on the conditional branch of \mathbf{G} , which is responsible to contribute the personalized features around the anchor prompt p .

We therefore find that for effective personalization of face image restoration, text-based pivoting alone is not enough, and that \mathbf{E} must be fine-tuned in conjunction with \mathbf{G}_p .

Step-2 - Model-based Pivoting. We are introducing a second fine-tuning step for \mathbf{E} within the context of \mathbf{G}_p . Essentially, our objective is to fine-tune \mathbf{E} in a way that it relinquishes identity cues to the personalized prior in \mathbf{G}_p while focusing on other detail cues. In this scenario, our pivot is not a text but a network (\mathbf{G}_p), which we keep fixed during the optimization process to align the encoder with the personalized prior.

To preserve the identity-agnostic role of the guiding encoder, we intentionally aim to avoid personalizing it. One approach to achieve this is by updating \mathbf{E} across different individuals, allowing it to adapt to the conditional branch of \mathbf{G}_p while remaining agnostic to fine-grained identity features, which should be determined by \mathbf{G}_p , as demonstrated in Fig. 4. This identity-agnostic retargeting concept bears similarities to the Prior Preservation loss [35] in the context of pivotal-tuning around a model.

Mathematically, with \mathbf{G}_p as our starting point, we perform fine-tuning on \mathbf{E} as follows:

$$\mathbf{B}_p = \mathcal{P}\{\mathbf{B}_E = \{\mathbf{G}_p, \mathbf{E}\}, \mathbf{G}_p\}, \quad (7)$$

where \mathbf{B}_E represents the restoration system (with the embedded personalized prior), and we are now optimizing the weights of \mathbf{E} .

3.4. Speeding-Up Dual-Pivot Tuning

In general, personalization of generative models is a time-consuming endeavor. Given our dual pivot tuning approach, personalization involves two finetuning steps per identity: textual pivoting, followed by model-based pivoting. Hence we next suggest steps to significantly reduce (by about 2x) fine-tuning time of each pivot tuning.

Speeding up textual pivoting. The presence of both conditional and unconditional branches within our inference pipeline affords an additional unique opportunity. We noticed that the initial steps of the restoration do not rely on identity as much, as these steps largely focus on coarse geometry and semantic detail [42]. Therefore, during inference, we observe that high-quality, identity-preserving restoration can be achieved even when the initial denoising steps are only unconditional, using a guidance scale of 0, followed by text-guided denoising for later steps with a non-zero guidance scale. This is mathematically represented as follows:

$$\begin{aligned} \epsilon_{t+1} &= \mathbf{B}_p(\mathbf{x}_t, \emptyset) \mid t < \gamma, \\ \epsilon_{t+1} &= w \cdot \mathbf{B}_p(\mathbf{x}_t, p) + (1 - w) \mathbf{B}_p(\mathbf{x}_t, \emptyset) \mid \gamma \leq t < 1.0, \end{aligned} \quad (8)$$

where γ denotes the fraction of denoising steps for which unconditional inference is carried out. Note that in the

above expression, we denote the initial noise to be at $t = 0$ and the restored image to be at $t = 1$.

We demonstrate this in Fig. 5, where we restore the degraded image (a) unconditionally for the first $\gamma = 50\%$ of steps, and conditionally for the remaining steps (c). Despite this, we find the restored image being faithful to the reference image (d), as well as to the restored image obtained through conditional restoration for all the steps (b). $\gamma = 50\%$ is identified experimentally. This observation enables us to reduce personalization time for the textual pivoting by about 2x since the denoiser no longer needs to be personalized for higher noise levels (since the unconditional model suffices for those), and can, therefore, be trained with a focus on relatively lower noise levels.

Speeding up model-based pivoting. Coupling the generative prior \mathbf{G} and the guiding encoder \mathbf{E} during the textual pivoting step can provide encoder context to the personalized generative prior. To achieve this, we propose to fine-tune \mathbf{G} within the context of \mathbf{B} , while pivoting around the prompt p , such that it leverages the conditioning cues from \mathbf{E} , namely,

$$\mathbf{B}_p = \mathcal{P}\{\mathbf{B}_G, p\}, \quad (9)$$

where \mathbf{B}_G denotes that we modify the weights of \mathbf{G} within the context of \mathbf{B} . Specifically, this personalization pivots around the text prompt p in the context of image restoration. The performance of this so-called in-context textual pivoting, and comparison with the previously discussed out-of-context textual pivoting is shown in Fig. 10 and discussed in detail later: while in-context textual pivoting improves identity information in the restored images, model-based pivoting is still required to retarget the encoder.

With the personalization of the generative prior being in-context in our proposed pipeline, we find that the model-based pivoting is feasible with half the number of finetuning steps, when compared with an out-of-context textual pivoting pipeline (Fig. 10). On an NVIDIA Tesla V100 GPU, this leads to a model-based pivoting time of about 10 minutes, as compared to 20 minutes in the case of out-of-context textual pivoting.

In practice, we have observed that the personalized prior in \mathbf{G}_p is sufficiently strong, such that even when performing the model-based pivoting of \mathbf{E} on a single individual, \mathbf{E} is retargeted to capture general cues and can be shared across various identities, as demonstrated in Fig. 6. This is critical from a training time perspective: the model-based pivoting, once performed on one identity, can be shared across models for different identities. Therefore, the only personalization step needed for each identity is the textual pivoting.

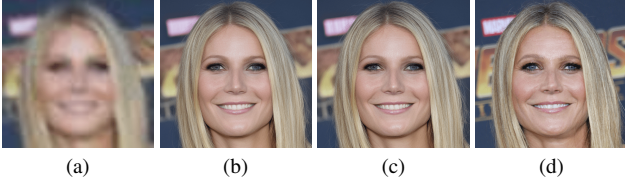


Figure 5. **Unconditional Sampling.** We found that during inference, identity-preserved restoration is possible even with unconditional denoising for initial steps, followed by conditional denoising for the remaining steps. For a degraded input (a), we use unconditional sampling for the first 50% of steps, followed by conditional sampling for the remaining steps (c). We find this to still be consistent with the reference image (d), both in terms of identity as well as faithfulness to the original image, as well as with the restored image using conditional restoration for all the steps (b).

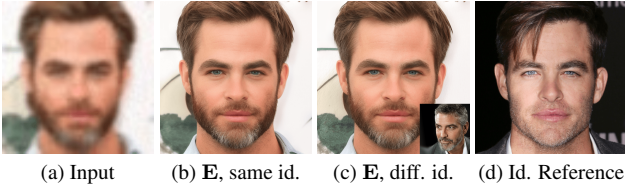


Figure 6. **Finetuning E on different identities.** We show that for the model-based pivot tuning E can be finetuned on the same identity (b), as well as on different identities as in the inset (c), while providing similar plausible restorations with respect to the identity in the reference image (d).

4. Experiments

In this section, we show through qualitative and quantitative analysis that the proposed method is superior to prior reference-based and blind image restoration methods.

4.1. Training Process and Datasets

We use images from CelebRef-HQ dataset [24] to personalize the model; more specifically, this dataset has $> 10\,512 \times 512$ images of the same person with 500 identities, and each time we use one identity’s images. Our method is trained on synthetic data that covers a wide range of degradation similar to the real world.

We follow the same second-order degradation strategy as [25]. At each stage we first convolve the image with a blur kernel k_σ , and downsample with a scale factor r . Following that, additive noise n_δ is added, and finally the image is JPEG-compressed with quality q . Formally, a single stage can be described as

$$\mathbf{x}_d = [(\mathbf{x} \otimes k_\sigma) \downarrow_r + n_\delta]_{\text{JPEG}_q}, \quad (10)$$

where \otimes is the convolution operator. The final image is obtained after applying Eq. (10) twice. We refer you to [25] for more details on the degradation process.

Table 1. **Fidelity and identity metrics.** The proposed method generates images with high fidelity, while showing superior identity retention, when personalized on 10 images. We compare along PSNR and SSIM as fidelity metrics, while the ArcFace similarity serves as an identity metric.

Method	PSNR (dB)	SSIM	ArcFace (Identity)
GFPGAN [46]	23.67	0.58	0.75
CodeFormer [56]	23.98	0.57	0.76
MyStyle [29]	17.24	0.53	0.68
DR2 [49]	21.56	0.54	0.40
ASFFNet [22]	11.21	0.40	0.55
DMDNet [24]	11.33	0.40	0.61
DiffBIR [25]	24.27	0.58	0.76
Ours	23.72	0.55	0.88

Test data We did test on three datasets: (1) CelebRef-HQ test set, (2) Google searched images including low-quality and high-quality images from the same person, (3) our collected real data from acquaintance.

4.2. Comparisons with other strategies

We show the comparisons of our personalization strategy to the alternative strategies in Fig. 2. As can be seen, the proposed strategy maximizes identity preservation through the restoration process, while comparison strategies, namely personalizing when pivoting only on the text condition (c) or personalizing when pivoting only on the generative model both are unable to effectively incorporate identity while retaining image fidelity.

4.3. Comparisons with SOTA methods

We perform qualitative and quantitative comparisons between our method and several state-of-the-art reference-based and blind face image restoration methods. For reference-based methods, we chose ASFFNet [23], DMDNet [24], and MyStyle [29]; for a fair comparison, all methods use 10 reference images for guidance. For blind face image restoration, we chose DiffBIR [25], DR2 [49], GFP-GAN [46], and CodeFormer [56]. For ease of reading, we put qualitative results from MyStyle, DR2, GFP-GAN, and CodeFormer in the appendix.

Comparison on synthetic degradations. Fig. 7 and Fig. E show qualitative comparisons of the methods on the CelebRef-HQ test set subject to the synthetic degradations described above. It is noteworthy that ASFFNet and DMDNet are trained on perfectly aligned face images. During test time, highly accurate face alignment is required to eliminate domain gap and get high-quality restoration results, which is hard to achieve on severely degraded images. As a result, the results of both methods are underwhelming. On the other hand, diffusion-based methods (DiffBIR and ours) are possess a generative prior trained on huge amount of un-



Figure 7. **Results on synthetically degraded images.** A considerable shift in identity can be observed between our proposed method and alternative baselines. Identity preservation can be observed in terms of overall geometric features, as well as attributes: eye shape (row 1), unnatural mole on the chin in the DiffBIR result (row 2), teeth structure and shape (row 3), eye color and feature between eyes (row 4), nose and nostrill shape (row 5), eye color (row 6).

aligned faces and can generalize well on test images without specific alignment, which leads to significantly higher restoration quality. MyStyle, which relies on a personalized generative prior, shows very good identity retention, however the restored images lack fidelity to the input degraded

image. Blind restoration techniques, such as CodeFormer, GFP-GAN and DiffBIR lead to significant identity drifts, while retaining fidelity to the input image. Compared to DiffBIR, our method achieves better fidelity to the ground truth face details, especially in terms of eye shape, eye color,

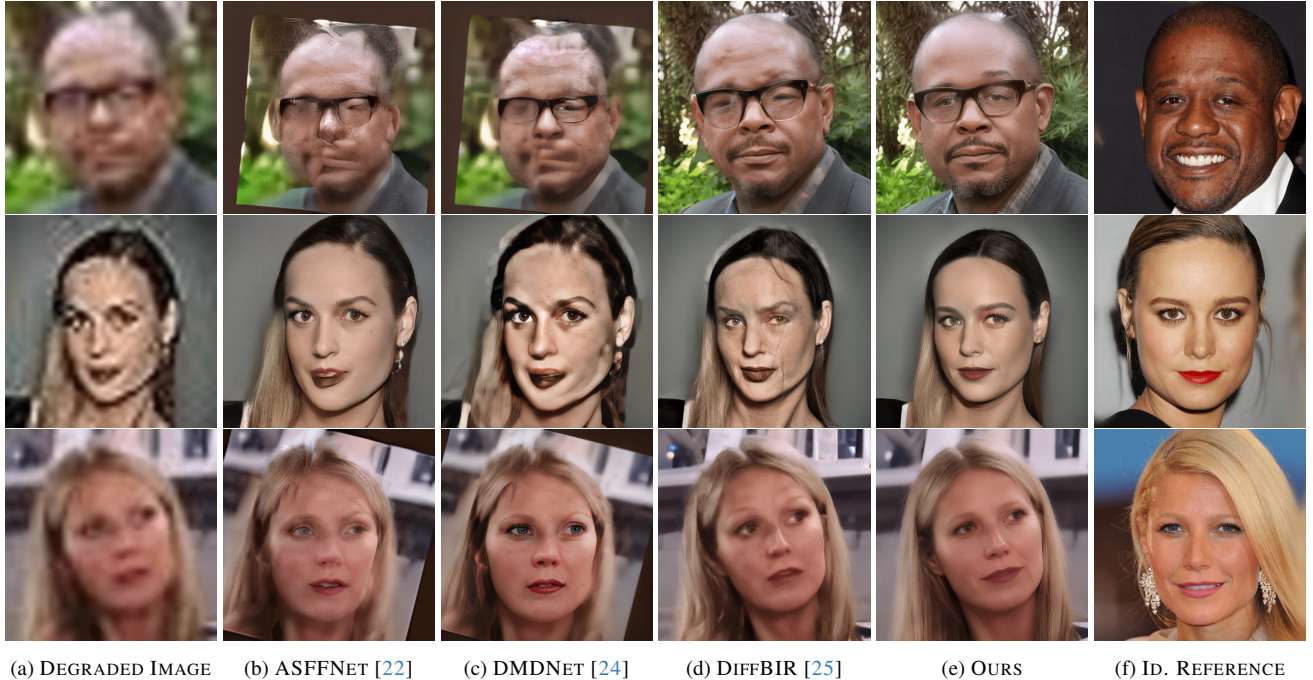


Figure 8. **Results on real degraded images.** It can be seen that even in images in the wild with real, unknown degradation kernels, our proposed method is superior to the baselines in terms of identity retention while maintaining high fidelity to the degraded input.



Figure 9. **Our approach is agnostic to different types of degradation, such as blur (top row), compression (middle row).** Prior face image restoration methods (b, c) have their estimates considerably affected by the nature of the degradation (note artifacts near eyes and mouth). Prior unconditional diffusion methods (d) have more consistent performance, but with lost identity information (note **eye shape**, **nose shape**). Our proposed method provides consistent restoration across a range of degradations, while retaining identity.

nose shapes and eyebrows, demonstrating that the proposed method can indeed better preserve identities.

In addition to qualitative comparisons, we also report the quantitative results on the entire CelebRef-HQ test set in Tab. 1. We report PSNR and SSIM as full-reference metrics. To quantify the identity disparity from the ground truth image, we use ArcFace [10] similarity. As observed in the

qualitative comparisons, ASFFNet and DMDNet cannot restore the images effectively, resulting in low scores on all the metrics. On the other hand, MyStyle results in poor quantitative performance, even through the qualitative results show restored images with high fidelity. This can be attributed to the lack of faithfulness of the restored image to the input image. The blind restoration methods (GFP-

GAN, CodeFormer, DR2 and DiffBIR) show varying degrees of performance, however DiffBIR is found to perform the best among these. Our method achieves higher identity preservation, at the cost of slightly lower PSNR and SSIM to DiffBIR. One explanation is that while DiffBIR tends to generate smooth restorations to which PSNR and SSIM are not sensitive, our method injects realistic high-frequency details that may not be perfectly aligned with the ground truth image, thus decreasing the scores. In summary, across all compared methods, the proposed method is still able to provide high image fidelity, while retaining identity. Some additional notes on the baseline qualitative metrics may be found in Sec. B.

We also conduct a user study to identify the perceptual benefit of our contextual personalized prior (Appendix Sec. B). We make two important observations: first, comparing unpersonalized diffusion-based face restoration [25] with our personalized method, a large majority of participants in our study note that personalization in fact improves identity-independent image quality as well. Second, we analyze the benefit of our personalized prior towards perceived identity retention while being faithful to the input image. Specifically, we note that the proposed method is predominately found to be superior, when compared with unconditional diffusion-based image restoration [25], reference-based image restoration [56], and GAN-based personalized priors [29].

Comparison on real degradations. Fig. 8 and Fig. F shows the performance of each method on real-world images. For each test image, the model is personalized with 10 reference images of the same identity from CelebRef-HQ. We also provide a reference image in column (f) for better evaluation of the identity preservation. This set of experiments show that our personalized model generalizes well to real-world degraded images. In all cases, our method achieves significantly better image quality than ASFFNet DMDNet, GFP-GAN and CodeFormer, and preserves identity better than DiFFBIR. When compared with MyStyle, in this operating regime the proposed method is considerably more faithful to the input degraded image, while being able to retain identity.

Consistent restoration through personalized prior. To show the strength of our personalized prior, we conduct an experiment by applying different synthetic degradations on the same image and observe how each method restores them, as shown in Fig. 9. The upper row shows a blurring degradation, while the lower row shows a compression degradation. For ASFFNet and DMDNet, the quality of the restored images varies with the degradations being applied. DiffBIR generates higher quality images, but the identity remains sensitive to the input degraded image. For example, in Fig. 9(d), note the inconsistent eye and nose shape, when compared with Fig. 9(f). Our personalized model effec-

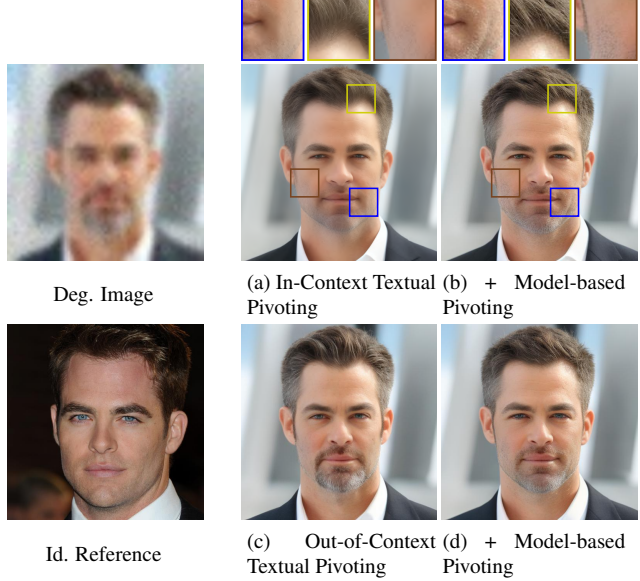


Figure 10. **Ablation: understanding dual-pivot tuning.** (a) In-context textual pivoting enables identity injection, however there still remains a gap in both identity and quality. This is bridged through the model-based pivoting (b). Note the difference in texture information within the insets, for features such as hair (yellow) and beard (blue, brown). Please zoom in for a clearer distinction. This can be compared with the alternative proposed approach. By beginning with out-of-context textual pivoting (c), significant drifts in identity are seen (note the eye shape) as the restoration pipeline is unable to leverage the personalized prior. However in this setting, the effect of the model-based pivoting is much more pronounced (d): alignment of \mathbf{E} with the personalized prior leads to significant improvement in identity preservation, and comparable performance with the upper row.

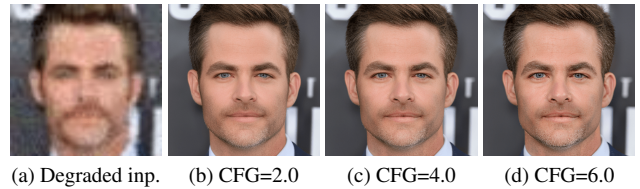


Figure 11. **Effect of classifier free guidance (CFG).** Sweeping across CFG enables a fidelity-diversity tradeoff, also manifesting as a tradeoff between image sharpness with realism (higher the CFG, higher the sharpness). This provides a degree of user control.

tively restores the images with consistent perceptual quality and identity fidelity. This indicates the stability of the contextual prior and the reliability of the encoder conditioning, across degradation types.

Ablation: Understanding Dual-Pivot Tuning. We find the proposed dual-pivot tuning approach to be a general technique for personalization of guided diffusion models. Fig. 10 qualitatively explores the benefits of this method.

Specifically in our case, we find that alternate strategies for personalization exist. The first is our chosen strategy: in-context textual pivoting (Fig. 10(a)), which injects identity information, followed by model-based pivoting (Fig. 10(b)), which enables better utilization of the general restoration prior to get high-fidelity restored images. The alternate approach involves beginning with out-of-context textual pivoting (where \mathbf{G} is personalized outside the context of \mathbf{B}). As shown in Fig. 10(c), this step leads to significant gap in identity as the restoration pipeline is unable to utilize the newly injected identity information. However, post the model-based pivoting (Fig. 10(d)), this is resolved, leading to high fidelity, identity preserving image restoration. The dual-pivot tuning approach successfully personalized the diffusion model in both these settings. As discussed previously, we find the in-context textual pivoting to enable faster personalization in terms of the the model-based pivoting step.

Classifier-free guidance scale. Fig. 11 shows an ablation study on the effect of classifier-free guidance scale. As can be seen, the parameter allows for trading off image sharpness with realism, allowing for preference-based tuning. Specifically, we find that increasing the CFG scale makes the restored images sharper, at the cost of realism (additional quantitative analysis in Appendix Sec. D). We also note in Fig. 5 that the proposed method does not require conditional inference across all denoising steps. That is, to enable personalized restoration, we find that even though initial denoising steps are carried out unconditionally, effective personalized restoration is possible.

Additional Applications: Fig. 12 shows the ability of our personalized generative prior to enable applications such as face swapping (top row) and text-guided editing (bottom row). Specifically, we blur the source image to obscure identity. Then, for face swapping we follow by restoration using the personalized prior for a new identity, then stitching the restored face back to the unblurred, original image. In the text-guided editing application we utilize the semantic prior of the diffusion model for text-conditional editing of the restored image. For example, with the term “smiling” as part of the prompt, we see a smile in the expression of the individual in the output image. In addition, with the phrase “blue”, “green” or “yellow eyes”, we see a clear variation in the eye color. Please zoom in for clearer visualization.

5. Conclusion

We propose a technique for personalizing a diffusion prior for face image restoration, leveraging the capabilities of few-shot fine-tuning based on a set of example images of the person. Our method achieves high fidelity to both the input image and the identity of the person. We conduct extensive experiments to demonstrate the superiority of our method in comparison to various state-of-the-art alterna-

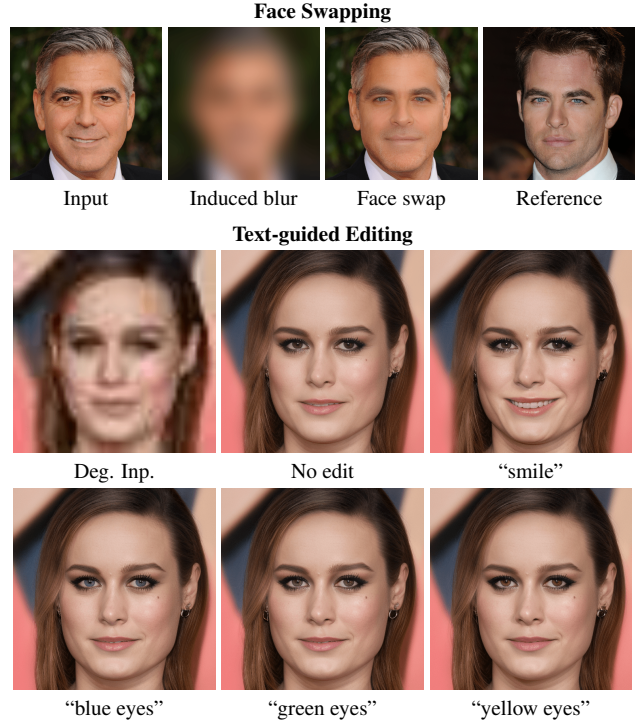


Figure 12. **Editing applications: face swapping text-guided editing.** The upper row shows the application of face swapping, while the lower row shows performance on text-guided editing.

tives for both blind and few-shot personalized face image restoration methods.

Limitations and Future Work. Although we make the very first step in using contextually personalized diffusion prior for face image restoration, it requires a computationally consuming fine-tuning process for each identity, which limits its deployability in large-scale systems. An important research direction is to inject few-shot identity in a feed-forward way, which we leave for future work. Furthermore, we would like to point out that, while the personalized model has improved fidelity to the identity, its general fidelity and quality are fundamentally limited by the underlying restoration method. Even though improving general quality is not the focus of this work, we believe the idea of contextual personalization holds promise for application in forthcoming restoration methods, achieving improved performance in both image quality and identity fidelity. Additionally, potential limitations native to personalization [35] on a small set of images can find their way to our method as well: namely overfitting towards features such as open eyes and smiling mouth if most of the training images show this, and the input degraded image is ambiguous in this aspect.

Acknowledgements. We thank Jackson Wang and Fangzhou Mu for helpful discussions and feedback on this manuscript.

References

- [1] Yuval Alaluf, Elad Richardson, Gal Metzer, and Daniel Cohen-Or. A neural space-time representation for text-to-image personalization. *arXiv preprint arXiv:2305.15391*, 2023. 3
- [2] Moab Arar, Rinon Gal, Yuval Atzmon, Gal Chechik, Daniel Cohen-Or, Ariel Shamir, and Amit H Bermano. Domain-agnostic tuning-encoder for fast personalization of text-to-image models. *arXiv preprint arXiv:2307.06925*, 2023. 4
- [3] Omri Avrahami, Kfir Aberman, Ohad Fried, Daniel Cohen-Or, and Dani Lischinski. Break-a-scene: Extracting multiple concepts from a single image. *arXiv preprint arXiv:2305.16311*, 2023. 4
- [4] Tim Brooks, Aleksander Holynski, and Alexei A Efros. Instructpix2pix: Learning to follow image editing instructions. In *Proceedings of the IEEE/CVF Conference on Computer Vision and Pattern Recognition*, pages 18392–18402, 2023. 4
- [5] Adrian Bulat and Georgios Tzimiropoulos. Super-fan: Integrated facial landmark localization and super-resolution of real-world low resolution faces in arbitrary poses with gans. In *Proceedings of the IEEE Conference on Computer Vision and Pattern Recognition*, pages 109–117, 2018. 3
- [6] Kelvin CK Chan, Xintao Wang, Xiangyu Xu, Jinwei Gu, and Chen Change Loy. Glean: Generative latent bank for large-factor image super-resolution. In *Proceedings of the IEEE/CVF conference on computer vision and pattern recognition*, pages 14245–14254, 2021. 3
- [7] Chaofeng Chen, Xiaoming Li, Lingbo Yang, Xianhui Lin, Lei Zhang, and Kwan-Yee K Wong. Progressive semantic-aware style transformation for blind face restoration. In *Proceedings of the IEEE/CVF Conference on Computer Vision and Pattern Recognition*, pages 11896–11905, 2021. 3
- [8] Wenhui Chen, Hexiang Hu, Yandong Li, Nataniel Ruiz, Xuhui Jia, Ming-Wei Chang, and William W Cohen. Subject-driven text-to-image generation via apprenticeship learning. *arXiv preprint arXiv:2304.00186*, 2023. 3
- [9] Yu Chen, Ying Tai, Xiaoming Liu, Chunhua Shen, and Jian Yang. Fsrnet: End-to-end learning face super-resolution with facial priors. In *Proceedings of the IEEE Conference on Computer Vision and Pattern Recognition*, pages 2492–2501, 2018. 3
- [10] Jiankang Deng, Jia Guo, Niannan Xue, and Stefanos Zafeiriou. Arcface: Additive angular margin loss for deep face recognition. In *Proceedings of the IEEE/CVF conference on computer vision and pattern recognition*, pages 4690–4699, 2019. 9
- [11] Prafulla Dhariwal and Alexander Nichol. Diffusion models beat gans on image synthesis. *Advances in neural information processing systems*, 34:8780–8794, 2021. 3
- [12] Berk Dogan, Shuhang Gu, and Radu Timofte. Exemplar guided face image super-resolution without facial landmarks. In *The IEEE Conference on Computer Vision and Pattern Recognition (CVPR) Workshops*, 2019. 3
- [13] Rinon Gal, Yuval Alaluf, Yuval Atzmon, Or Patashnik, Amit H Bermano, Gal Chechik, and Daniel Cohen-Or. An image is worth one word: Personalizing text-to-image generation using textual inversion. *arXiv preprint arXiv:2208.01618*, 2022. 2, 3
- [14] Rinon Gal, Moab Arar, Yuval Atzmon, Amit H Bermano, Gal Chechik, and Daniel Cohen-Or. Encoder-based domain tuning for fast personalization of text-to-image models. *ACM Transactions on Graphics (TOG)*, 42(4):1–13, 2023. 4
- [15] Yuchao Gu, Xintao Wang, Liangbin Xie, Chao Dong, Gen Li, Ying Shan, and Ming-Ming Cheng. Vqfr: Blind face restoration with vector-quantized dictionary and parallel decoder. *arXiv preprint arXiv:2205.06803*, 2022. 3
- [16] Jonathan Ho and Tim Salimans. Classifier-free diffusion guidance. *arXiv preprint arXiv:2207.12598*, 2022. 4
- [17] Jonathan Ho, Ajay Jain, and Pieter Abbeel. Denoising diffusion probabilistic models. *Advances in neural information processing systems*, 33:6840–6851, 2020. 3
- [18] Bahjat Kavar, Shiran Zada, Oran Lang, Omer Tov, Huiwen Chang, Tali Dekel, Inbar Mosseri, and Michal Irani. Imagic: Text-based real image editing with diffusion models. In *Proceedings of the IEEE/CVF Conference on Computer Vision and Pattern Recognition*, pages 6007–6017, 2023. 4
- [19] Deokyun Kim, Minseon Kim, Gihyun Kwon, and Dae-Shik Kim. Progressive face super-resolution via attention to facial landmark. *arXiv preprint arXiv:1908.08239*, 2019. 3
- [20] Xiaoming Li, Ming Liu, Yuting Ye, Wangmeng Zuo, Liang Lin, and Ruigang Yang. Learning warped guidance for blind face restoration. In *The European Conference on Computer Vision (ECCV)*, 2018. 3
- [21] Xiaoming Li, Chaofeng Chen, Shangchen Zhou, Xianhui Lin, Wangmeng Zuo, and Lei Zhang. Blind face restoration via deep multi-scale component dictionaries. In *European Conference on Computer Vision*, pages 399–415. Springer, 2020. 3
- [22] Xiaoming Li, Wenyu Li, Dongwei Ren, Hongzhi Zhang, Meng Wang, and Wangmeng Zuo. Enhanced blind face restoration with multi-exemplar images and adaptive spatial feature fusion. In *CVPR*, 2020. 7, 8, 9, 16, 19, 20
- [23] Xiaoming Li, Wenyu Li, Dongwei Ren, Hongzhi Zhang, Meng Wang, and Wangmeng Zuo. Enhanced blind face restoration with multi-exemplar images and adaptive spatial feature fusion. In *Proceedings of the IEEE/CVF Conference on Computer Vision and Pattern Recognition*, pages 2706–2715, 2020. 2, 3, 7
- [24] Xiaoming Li, Shiguang Zhang, Shangchen Zhou, Lei Zhang, and Wangmeng Zuo. Learning dual memory dictionaries for blind face restoration. *IEEE Transactions on Pattern Analysis and Machine Intelligence*, 2022. 2, 3, 7, 8, 9, 15, 16, 19, 20
- [25] Xinqi Lin, Jingwen He, Ziyang Chen, Zhaoyang Lyu, Ben Fei, Bo Dai, Wanli Ouyang, Yu Qiao, and Chao Dong. Diffbir: Towards blind image restoration with generative diffusion prior. *arXiv preprint arXiv:2308.15070*, 2023. 1, 2, 3, 4, 5, 7, 8, 9, 10, 15, 16, 17, 19, 20
- [26] Zhiheng Liu, Ruili Feng, Kai Zhu, Yifei Zhang, Kecheng Zheng, Yu Liu, Deli Zhao, Jingren Zhou, and Yang Cao. Cones: Concept neurons in diffusion models for customized generation. *arXiv preprint arXiv:2303.05125*, 2023. 4
- [27] Xuan Luo, Xuaner Zhang, Paul Yoo, Ricardo Martin-Brualla, Jason Lawrence, and Steven M Seitz. Time-travel

- rephotography. *ACM Transactions on Graphics (TOG)*, 40(6):1–12, 2021. 3
- [28] Chong Mou, Xintao Wang, Liangbin Xie, Yanze Wu, Jian Zhang, Zhongang Qi, Ying Shan, and Xiaohu Qie. T2i-adapter: Learning adapters to dig out more controllable ability for text-to-image diffusion models. *arXiv preprint arXiv:2302.08453*, 2023. 4
- [29] Yotam Nitzan, Kfir Aberman, Qiurui He, Orly Liba, Michal Yarom, Yossi Gandelsman, Inbar Mosseri, Yael Pritch, and Daniel Cohen-Or. Mystyle: A personalized generative prior. *ACM Transactions on Graphics (TOG)*, 41(6):1–10, 2022. 2, 3, 7, 10, 15, 16, 17, 18, 19, 20
- [30] Ryan Po, Guandao Yang, Kfir Aberman, and Gordon Wetzstein. Orthogonal adaptation for modular customization of diffusion models. *arXiv preprint arXiv:2312.02432*, 2023. 4
- [31] Ryan Po, Wang Yifan, Vladislav Golyanik, Kfir Aberman, Jonathan T Barron, Amit H Bermano, Eric Ryan Chan, Tali Dekel, Aleksander Holynski, Angjoo Kanazawa, et al. State of the art on diffusion models for visual computing. *arXiv preprint arXiv:2310.07204*, 2023. 3
- [32] Aditya Ramesh, Prafulla Dhariwal, Alex Nichol, Casey Chu, and Mark Chen. Hierarchical text-conditional image generation with clip latents. *arXiv preprint arXiv:2204.06125*, 2022. 3
- [33] Daniel Roich, Ron Mokady, Amit H Bermano, and Daniel Cohen-Or. Pivotal tuning for latent-based editing of real images. *ACM Transactions on graphics (TOG)*, 42(1):1–13, 2022. 4
- [34] Robin Rombach, Andreas Blattmann, Dominik Lorenz, Patrick Esser, and Björn Ommer. High-resolution image synthesis with latent diffusion models. In *Proceedings of the IEEE/CVF conference on computer vision and pattern recognition*, pages 10684–10695, 2022. 2, 3, 4
- [35] Nataniel Ruiz, Yuanzhen Li, Varun Jampani, Yael Pritch, Michael Rubinstein, and Kfir Aberman. Dreambooth: Fine tuning text-to-image diffusion models for subject-driven generation. In *Proceedings of the IEEE/CVF Conference on Computer Vision and Pattern Recognition*, pages 22500–22510, 2023. 2, 3, 4, 6, 11
- [36] Nataniel Ruiz, Yuanzhen Li, Varun Jampani, Wei Wei, Tingbo Hou, Yael Pritch, Neal Wadhwa, Michael Rubinstein, and Kfir Aberman. Hyperdreambooth: Hypernetworks for fast personalization of text-to-image models. *arXiv preprint arXiv:2307.06949*, 2023. 4
- [37] Chitwan Saharia, William Chan, Saurabh Saxena, Lala Li, Jay Whang, Emily L Denton, Kamyar Ghasemipour, Raphael Gontijo Lopes, Burcu Karagol Ayan, Tim Salimans, et al. Photorealistic text-to-image diffusion models with deep language understanding. *Advances in Neural Information Processing Systems*, 35:36479–36494, 2022. 2, 3
- [38] Ziyi Shen, Wei-Sheng Lai, Tingfa Xu, Jan Kautz, and Ming-Hsuan Yang. Deep semantic face deblurring. In *Proceedings of the IEEE conference on computer vision and pattern recognition*, pages 8260–8269, 2018. 3
- [39] Yang Song, Jascha Sohl-Dickstein, Diederik P Kingma, Abhishek Kumar, Stefano Ermon, and Ben Poole. Score-based generative modeling through stochastic differential equations. In *International Conference on Learning Representations*, 2021. 3
- [40] Luming Tang, Nataniel Ruiz, Qinghao Chu, Yuanzhen Li, Aleksander Holynski, David E Jacobs, Bharath Hariharan, Yael Pritch, Neal Wadhwa, Kfir Aberman, et al. Realfill: Reference-driven generation for authentic image completion. *arXiv preprint arXiv:2309.16668*, 2023. 3
- [41] Yoad Tewel, Rinon Gal, Gal Chechik, and Yuval Atzmon. Key-locked rank one editing for text-to-image personalization. In *ACM SIGGRAPH 2023 Conference Proceedings*, pages 1–11, 2023. 3
- [42] Andrey Voynov, Qinghao Chu, Daniel Cohen-Or, and Kfir Aberman. $p+$: Extended textual conditioning in text-to-image generation. *arXiv preprint arXiv:2303.09522*, 2023. 3, 6
- [43] Jianyi Wang, Zongsheng Yue, Shangchen Zhou, Kelvin CK Chan, and Chen Change Loy. Exploiting diffusion prior for real-world image super-resolution. *arXiv preprint arXiv:2305.07015*, 2023. 2, 4, 5
- [44] Kaili Wang, Jose Oramas, and Tinne Tuytelaars. Multiple exemplars-based hallucination for face super-resolution and editing. In *Proceedings of the Asian Conference on Computer Vision*, 2020. 3
- [45] Su Wang, Chitwan Saharia, Ceslee Montgomery, Jordi Pont-Tuset, Shai Noy, Stefano Pellegrini, Yasumasa Onoe, Sarah Laszlo, David J Fleet, Radu Soricut, et al. Imagen editor and editbench: Advancing and evaluating text-guided image inpainting. In *Proceedings of the IEEE/CVF Conference on Computer Vision and Pattern Recognition*, pages 18359–18369, 2023. 4
- [46] Xintao Wang, Yu Li, Honglun Zhang, and Ying Shan. Towards real-world blind face restoration with generative facial prior. In *The IEEE Conference on Computer Vision and Pattern Recognition (CVPR)*, 2021. 3, 7, 17, 18, 19, 20
- [47] Zhihao Wang, Jian Chen, and Steven CH Hoi. Deep learning for image super-resolution: A survey. *IEEE transactions on pattern analysis and machine intelligence*, 43(10):3365–3387, 2020. 1
- [48] Zhouxia Wang, Jiawei Zhang, Runjian Chen, Wenping Wang, and Ping Luo. Restoreformer: High-quality blind face restoration from degraded key-value pairs. In *Proceedings of the IEEE/CVF Conference on Computer Vision and Pattern Recognition*, pages 17512–17521, 2022. 3
- [49] Zhixin Wang, Ziyang Zhang, Xiaoyun Zhang, Huangjie Zheng, Mingyuan Zhou, Ya Zhang, and Yanfeng Wang. Dr2: Diffusion-based robust degradation remover for blind face restoration. In *Proceedings of the IEEE/CVF Conference on Computer Vision and Pattern Recognition*, pages 1704–1713, 2023. 3, 7, 15, 16, 17
- [50] Lingbo Yang, Shanshe Wang, Siwei Ma, Wen Gao, Chang Liu, Pan Wang, and Peiran Ren. Hifacegan: Face renovation via collaborative suppression and replenishment. In *Proceedings of the 28th ACM International Conference on Multimedia*, pages 1551–1560, 2020. 3
- [51] Tao Yang, Peiran Ren, Xuansong Xie, and Lei Zhang. Gan prior embedded network for blind face restoration in the wild. In *Proceedings of the IEEE/CVF Conference on Com-*

- puter Vision and Pattern Recognition*, pages 672–681, 2021. 3
- [52] Xin Yu, Basura Fernando, Bernard Ghanem, Fatih Porikli, and Richard Hartley. Face super-resolution guided by facial component heatmaps. In *Proceedings of the European conference on computer vision (ECCV)*, pages 217–233, 2018. 3
 - [53] Zongsheng Yue and Chen Change Loy. Difface: Blind face restoration with diffused error contraction. *arXiv preprint arXiv:2212.06512*, 2022. 3, 16, 17
 - [54] Lvmin Zhang, Anyi Rao, and Maneesh Agrawala. Adding conditional control to text-to-image diffusion models. In *Proceedings of the IEEE/CVF International Conference on Computer Vision*, pages 3836–3847, 2023. 4
 - [55] Yang Zhao, Yu-Chuan Su, Chun-Te Chu, Yandong Li, Marius Renn, Yukun Zhu, Changyou Chen, and Xuhui Jia. Rethinking deep face restoration. In *Proceedings of the IEEE/CVF Conference on Computer Vision and Pattern Recognition*, pages 7652–7661, 2022. 3
 - [56] Shangchen Zhou, Kelvin Chan, Chongyi Li, and Chen Change Loy. Towards robust blind face restoration with codebook lookup transformer. *Advances in Neural Information Processing Systems*, 35:30599–30611, 2022. 3, 7, 10, 17, 18, 19, 20

Appendix

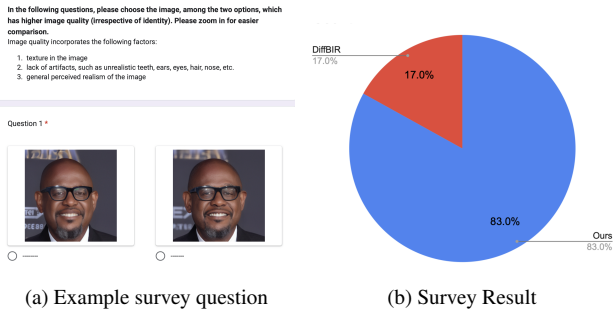


Figure A. **User study: effect of personalization on perceived image quality.** When asked to choose the image with better perceived quality, we find users predominantly choosing the images with our personalized restoration. Our method is indicated in blue, while DiffBIR [25] is shown in red, in the pie chart.

A. Appendix Contents

This appendix contains the following contents:

1. Additional quantitative analysis (Sec. B)
2. Additional qualitative analysis (Sec. C)
3. Additional observations (Sec. D)
4. Ethical considerations (Sec. E)

B. Additional Quantitative Analysis

Additional notes on Tab. 1. An interesting result to note is the performance of [49]. We note that DR2 allows for tunable parameters (N, τ) selection to tradeoff restoration with fidelity to the original image. We choose $(N, \tau) = (16, 35)$ as we find this combination able to restore the degradations in our synthetic images. However, this does come at a cost of fidelity to the input - this is reflected by low fidelity as well as identity metrics for DR2.

Another interesting observation is the performance of MyStyle [29] in terms of identity retention. We see that the ArcFace metric for MyStyle is similar to other blind restoration techniques. This is a somewhat surprising observation, since MyStyle uses a personalized prior for restoration. This may be explained as follows: while MyStyle indeed shows strong identity retention (as evidenced by qualitative results in Figs. E to H), the method is unable to retain fidelity (in terms of color, lighting, texture, makeup and even pose). All these factors can affect the perceived identity of the image from the perspective of the ArcFace metric, leading to this anomaly. On the other hand, the ArcFace metric is a valid comparison of identity retention with all other comparison methods, since they are able to retain fidelity with the input degraded image.

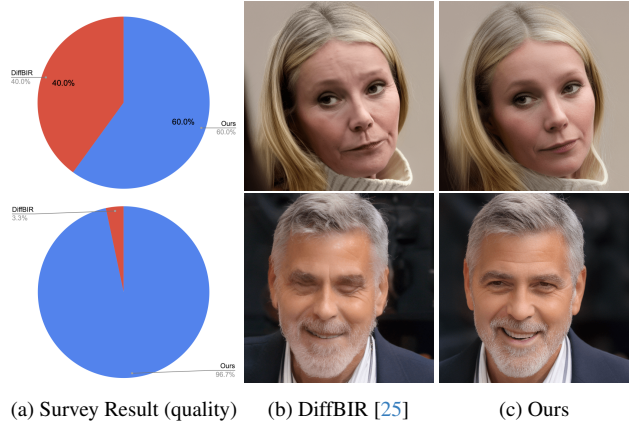


Figure B. **Two specific real degradation restorations, from the lens of image quality.** The upper row shows a case where respondent opinion is split - DiffBIR provides specific detail like wrinkles, while our approach provides structure and identity. The lower row shows a case with unanimous favor towards our method. This arises from specific artifacts in the DiffBIR output, which is avoided by having a strong personalized prior. Our method is indicated in blue, while DiffBIR [25] is shown in red, in the pie charts.

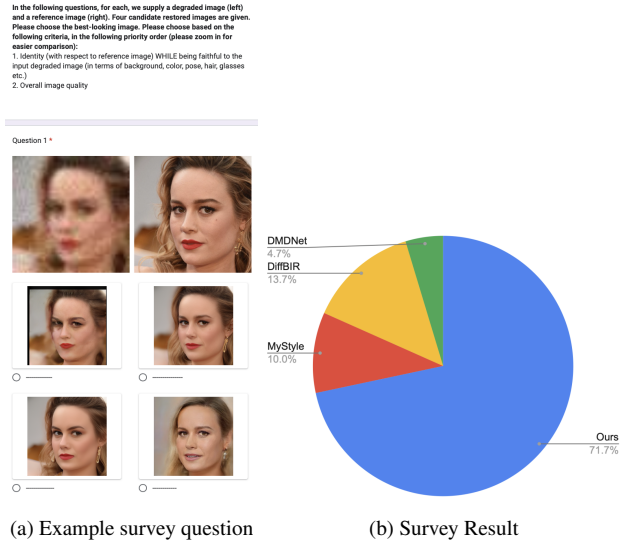


Figure C. **User study: the effect of personalization on perceived image identity retention.** When asked to choose the image with the better-looking image, while prioritizing identity and faithfulness to input degraded image, we find users predominantly choosing the images with our personalized restoration. Our method is indicated in blue, DiffBIR [25] is shown in yellow, MyStyle [29] is shown in red, and DMDNet [24] is shown in green in the pie chart.

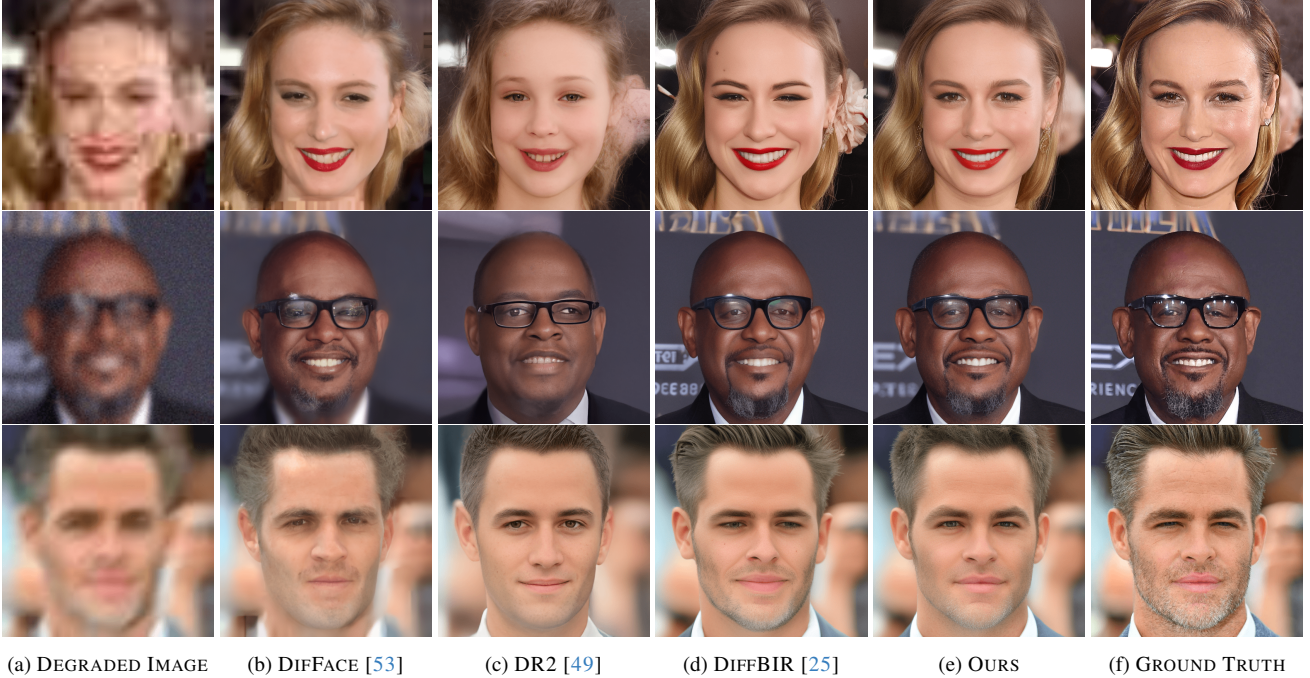


Figure D. **Comparison with existing diffusion-based blind image restoration methods.** We find that for the degree of degradation we deal with in our experiments, both DiffFace [53] as well as DR2 [49] show unreliable performance, losing both identity and fidelity at different instances. DiffBIR [25], on the other hand, while not performing as well as our method in terms of identity and fidelity retention, is the best performer among the prior diffusion-based methods. We therefore choose DiffBIR as our base model and comparison benchmark for subsequent experiments.

User study. We conduct a user study as a measure of perceptual quality and comparison with prior methods. We focus on two questions as part of the study: (a) can personalization help improve perceived image quality as well?, and (b) how does our method compare with prior methods in terms of identity-aware restoration. We perform our study across 30 participants. The survey consists of randomized, anonymized options that they can choose amongst. Figs. A and C (a) show the exact guidelines provided as part of the study. For part (a), image quality, we compare against the base unconditional restoration method (DiffBIR [25]), with the objective being to choose the better-quality image, irrespective of identity. For this case, we compare across 11 image pairs, containing both real and synthetic degradations. For part (b), identity-aware restoration, we compare with three methods: (i) DMDNet [24] (better-performing method both qualitatively and quantitatively when compared with ASFFNet [22]); (ii) MyStyle [29], a personalized generative prior; (iii) DiffBIR [25], a unconditional diffusion-based method. For this case, we compare across 10 image sets, consists of synthetically degraded images.

We begin with discussing the first part of the user study: effect of personalization on identity-independent perceived image quality. Fig. A shows the results of this part of the study. We observe that across the 30 study participants, a

clear majority of the participants indicate the quality improvement that arises out of personalization. This is an unexpected result, and we explore this further by analyzing two specific instances, in Fig. B. The upper row shows a case where the users are broadly split between the candidate options. The unconditional method provides a restored image with detailed facial features such as wrinkles, while the proposed method provides less of such detail, with stronger identity cues. Both images look viable as natural images with good quality. However, the lower row in Fig. B shows an instance where the study participants almost unanimously prefer our method. The reason for this is evident: the baseline method has considerable artifacts, especially near the eyes, while our method leads to a good quality, realistic face image. Through these observations, we can understand the effect of our personalization method on identity-independent image quality. In cases where the unconditional comparison method is able to perform, our personalized model remains stable and provides realistic looking faces. However, in cases where the comparison method fails, such as with high degradations, our method, through the strength of the identity prior, still results in realistic restored images. A combination of these two factors leads to superior perceived identity-independent image quality.

We next analyze the second part of the user study: the

perceived strength of our identity-aware image restoration. Fig. C shows the results of this part of the study. We see that, perhaps per expectation, participants rate our method as the predominant favorite in terms of identity-aware image restoration, while retaining faithfulness to the input degraded image. This can be seen across our various qualitative results and speaks to the strength and reliability of our personalized prior across identities and degradations. However, an interesting insight is the relative placement of the comparison methods. Specifically, study participants rate DiffBIR [25] to be the second-best method, despite not retaining identity, as a result of its strong correlation to the input degraded image. On the other hand, MyStyle [29], while having a strong identity prior, is the third-best preferred method on average, as a result of it not being faithful to the input image. That is, perceptually, faithfulness to the input degraded image is given a higher priority by participants, despite the study guidelines placing both identity and faithfulness to input image at the same priority.

C. Additional Qualitative Analysis

We now discuss additional qualitative results, comparing with a range of baselines. We first qualitatively compare our proposed method with existing diffusion-based blind restoration techniques. Specifically, we compare with DiffFace [53], DR2 [49] and DiffBIR [25]. Fig. D highlights these observations. We note that in our operating regime for degradation, both DR2 and DiffFace result in inaccurate and unreliable restoration (in both these cases, the models trade off fidelity with restoration and need to be used accordingly depending on the degree of degradation). In contrast, DiffBIR, while worse in both detail and identity when compared with our method, proves to be a much more reliable blind restoration technique. We therefore use DiffBIR as our base model for our method, and use it as the representative diffusion-based blind restoration technique in our analysis.

We next describe qualitative performance in comparison with GFPGAN [46] and CodeFormer [56] as blind image restoration methods, and MyStyle [29] as a method with a personalized generative prior, in additional detail to the paper. Fig. E shows results on synthetic degradations and corresponding restorations across six different identities. As can be seen, the blind restoration methods show clear drifts in identity across all six examples, while retaining fidelity to the input image. On the other hand, Nitzan et al. [29], while being able to retain a strong identity prior, sees a significant deviation in the restored image, from the input degraded image (potentially as a result of personalization on a small number of images (10)). In contrast, our method is able to achieve the best of both worlds: while maintaining a high degree of faithfulness to the input image, we also see consistent identity retention across all examples. This leads

to our results being closest to the reference image, despite the input having severe degradation in several cases.

We next look at Fig. F, for an analysis on real degraded images when compared with these additional baselines. Again, we note consistent observation. The blind restoration methods remain faithful to the input image, however they result in considerable identity drifts and artifacts in the restored images. MyStyle is able to continue retaining a strong personalized prior, however at the cost of losing all context relating to the input degraded image. Again, our method is able to retain identity, while being faithful to the input image.

Further, we supply additional synthetic (Fig. G) as well as real (Fig. H) degradation results across all baselines. We wish to highlight the robustness of our proposed method, across identities and degradations, over a larger number of image settings. These aspects can specifically be seen through identifying features in the participants, such as hair, teeth, ears, eye color and so on. The overall trends remain the same: prior methods are either able to retain strong identity without artifacts, or retaining faithfulness to the input image. It is through our personalization regime that we achieve the best of both these worlds, getting identity-consistent restored images with high fidelity.

D. Additional Observations

The Effect of Classifier Free Guidance. The qualitative effect of classifier free guidance (CFG) was discussed in the main paper (Figure 8). Here, we perform a quantitative analysis, through Tab. A. We note that traditional fidelity metrics worsen as the CFG is increased. This is consistent with our other observations, where the unconditional method (DiffBIR) shows slightly better performance on these metrics. As we increase the CFG, we move farther from the unconditional model and therefore see these effects. In terms of identity, we see a small reduction with increased CFG. This is also consistent with our observations from the main paper. As we increase the CFG, the sharpness of the restored image increases and may lead it to look unrealistic. Overall, in terms of traditional metrics, a lower CFG values is optimal. However, visually, the CFG can serve as a useful control knob for restored image style and quality, as discussed in Figure 8, main paper.

Dealing with Heavy Degradations. Fig. I shows a potentially interesting use setting for the proposed method. Namely, in the case of very heavy degradations, multiple passes through the restoration model may be performed. As seen in the figure, (b) is able to obtain coarse details as well as shape and structure information. Through a second pass, (c) is able to improve of texture and detail, in addition to obtaining greater identity injection, leading to a better restored image than (b).



Figure E. **Additional baseline methods on synthetically degraded images (in addition to the results in the main paper).** Similar observations to the synthetically degraded results can be made. The blind image restoration methods suffer both on identity and quality, while MyStyle is able to retain identity at the cost of losing faithfulness to the input image. Our method is able to retain identity in the restoration, while being faithful to the input image. In terms of specifics for each row, note the eye and eyebrow shape in row 1, eye shape, bags under the eyes, and teeth in row 2, eye shape and ears (specifically, left ear) in row 3, mole on the left cheek and mark between the eyes in row 4, eyes and mouth expression in row 5, and eye color in row 6. Please zoom in to observe these details more easily.

E. Ethical Considerations

The use of generative models, while being extremely helpful for challenging tasks such as identity-aware im-

age restoration, can also potentially have harmful effects. Specifically, generative models can be used for immoral tasks. In our case, applications that we discussed, such as

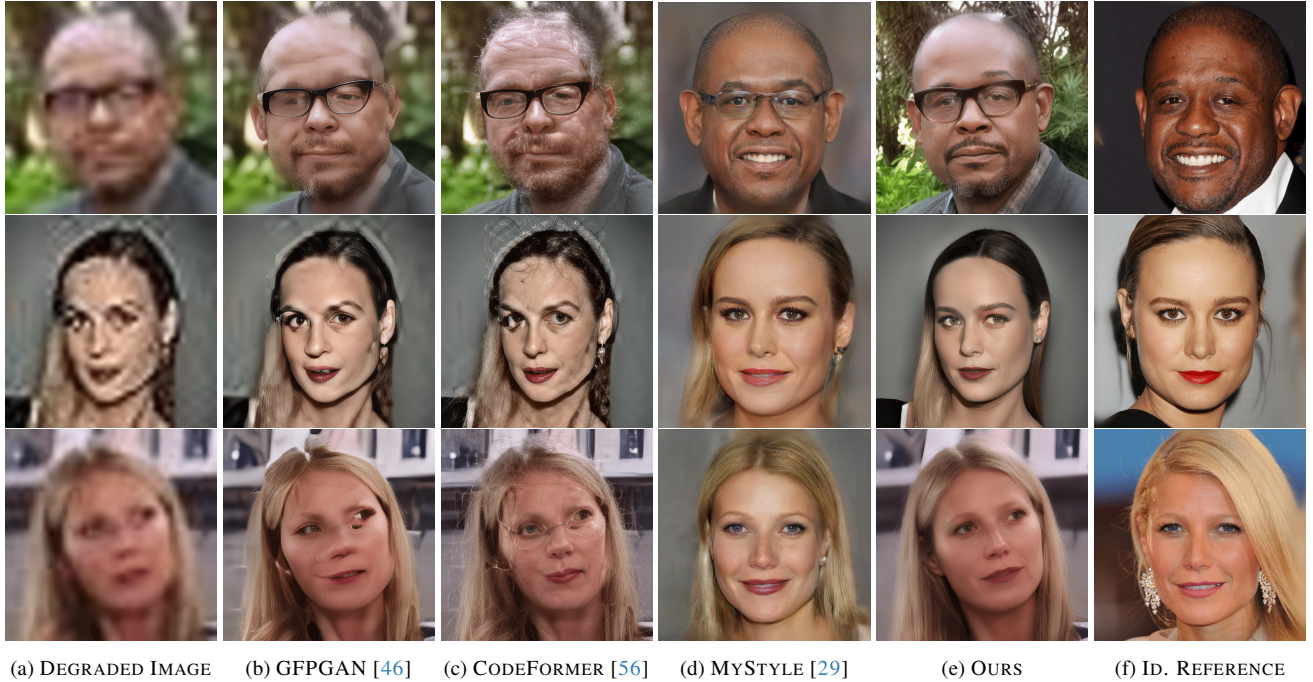


Figure F. **Additional baseline methods on real degraded images (in addition to the results in the main paper).** It can be seen that even in images in the wild with real, unknown degradation kernels, our proposed method is superior to the baselines in terms of identity retention while maintaining high fidelity to the degraded input. Comparison methods either result in artifacts or in an image that is not faithful to the input, while the proposed method is able to stably inject relevant identity information while retaining fidelity to the input degraded image. Please zoom in to the Figure for a clearer view.

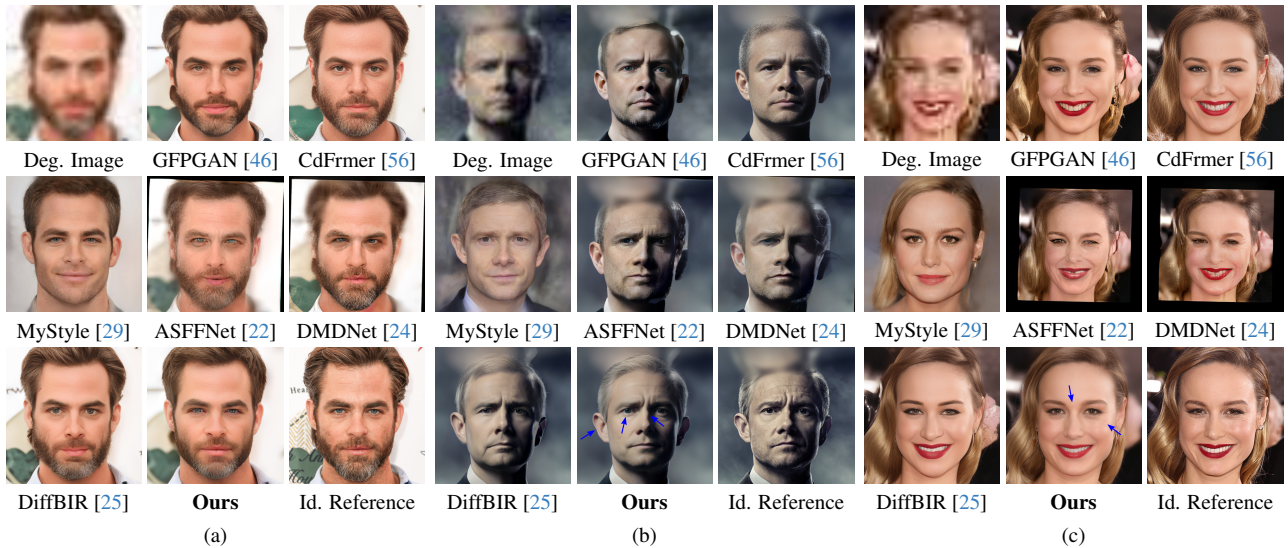


Figure G. **Additional results on synthetic degraded images, comparing with all discussed major comparison methods.** For identity (a), zooming in shows that all baseline methods either lead to considerable artifacts in the restored image, or through identity drifts (eye color) and lack of fidelity with the input image. For identity (b) in cases where the restored image does not have significant artifacts, identity drifts can be noted in the form of nose shape (as highlighted by the shadow on the nose), eye color and ear shape. For identity (c), the mark between the eyes and the mole on the left cheek are identifying features that show the superiority of the proposed method.

face swapping as well as text-guided editing, can lead to generation of fake images, that may be used without the

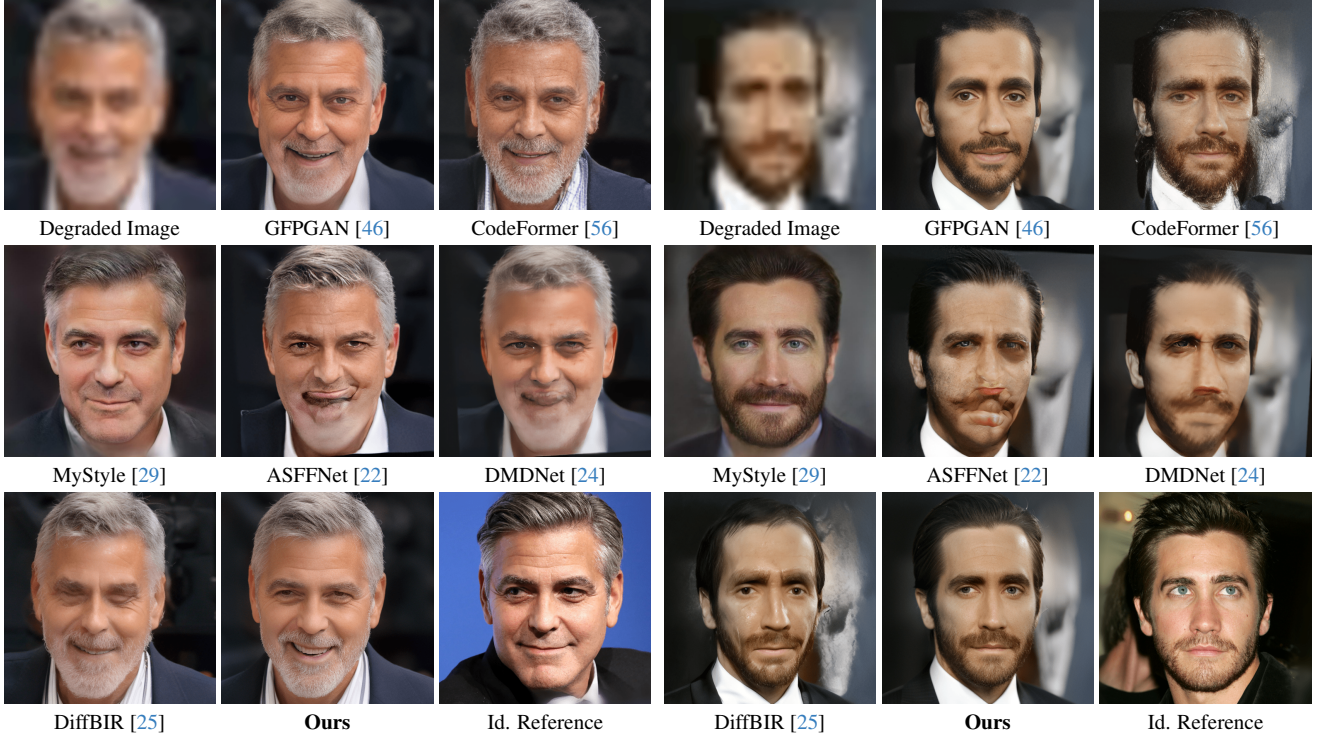


Figure H. **Additional results on real degraded images, comparing with all discussed major comparison methods.** For both identities, zooming in shows that comparison methods (both prior reference-based methods and blind restoration methods) result in strong artifacts, identity drifts, and in the case of MyStyle [29], lack of fidelity with the input degraded image. The proposed method is the only one consistently able to incorporate identity in the restoration in a stable manner. Please zoom in to the image for a clearer visualization.

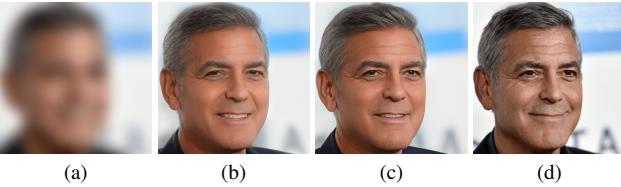


Figure I. **Heavy degradation restoration.** Given a highly degraded image (a), a first pass (b) through our restoration pipeline provides a coarse estimate that pulls the image closer to the input domain of the model. The second pass (c) injects texture and identity information, leading to a better restored estimate with respect to the ground truth (d).

consent of the person whose image it is. We strongly condemn such and any other use cases of the proposed method.

Table A. **Ablation: effect of classifier-free guidance scale on personalized image restoration.** We compare along PSNR and SSIM as fidelity metrics, while the ArcFace similarity serves as an identity metric.

CFG	PSNR (dB)	SSIM	ArcFace (Identity)
1.0	24.78	0.70	0.90
2.0	24.54	0.69	0.89
3.0	24.17	0.68	0.87
4.0	23.73	0.67	0.85
5.0	23.12	0.65	0.84